Acta Mech 224, 727–744 (2013)
DOI 10.1007/s00707-012-0772-3

Anil K. Vashishth · Ashok Dahiya

Shear waves in a piezoceramic layered structure

Received: 1 March 2012 / Revised: 10 August 2012 / Published online: 6 December 2012

Abstract The propagation of SH-type wave is studied in a composite structure consisting of alternating polymeric layers and porous piezoelectric layers. The porous piezoelectric materials of the composite structure are assumed to have 6 mm symmetry and their poling direction is along z-axis. Layers of the polymer are considered as isotropic dielectric elastic material. Solutions of the field equations for the porous piezoelectric material and for the polymeric material are obtained. Two cases, first when the direction of propagation of the SH-type wave is taken along the direction normal to the layering of the composite structure, and second when the propagation direction is taken along the layering, are considered for the derivation of the phase velocity. The dispersion and the stop-pass band behavior of the Floquet wave is also discussed. Numerical results for phase velocity and stop band effect are presented for a periodic system of alternating PZT-5H and polythene layers. The influence of volume fraction on phase velocity and stop band effect is discussed.

1 Introduction

Piezoelectric materials produce an electric field when deformed and undergo deformation when subjected to an electric field. Piezoelectric materials are integrated with structural systems to form a class of smart structures and are extensively used in various functional devices, such as sensors, actuators, filters and delay lines, medical appliances, SAW (surface acoustic wave) devices and others. Due to the brittle nature of piezoelectric ceramics and due to the possible defects of impurities, cavities and microcracks, failures of devices occur easily under mechanical and/or electrical loadings. However, the introduction of a controlled porosity into a piezoelectric material could strongly improve its acoustic performances and therefore its ultrasonic response. Materials containing tailored porosity exhibit special properties and features that usually cannot be achieved by their conventional dense counterparts. Therefore, porous piezoceramics find, nowadays, many applications as ultrasonic transducers. Composites are materials that are receiving growing attention by the scientific as well as the industrial world. They can, in fact, show specific properties (electronic, magnetic, mechanical, etc.) that cannot be achieved otherwise by single phase materials. This approach has been applied for the first time to piezoelectric materials at the end of the 1970s combining them with polymeric and/or metallic phases to obtain actuators or transducers. The development of such piezoelectric composites aims to combine the specific properties of each single phase to maximize the electromechanical and ultrasonic response of a particular device. Composites, consisting of porous piezoelectric ceramics and polymers, not only can eliminate the defects of strength and brittleness in pure piezoelectric ceramic, but also can increase its performance.

A. K. Vashishth (✉) · A. Dahiya
Department of Mathematics, Kurukshetra University, Kurukshetra 136119, India
E-mail: akvashishth@kuk.ac.in

The details of piezoelectric composite structures can be found in [1,2,4,5]. Shear horizontal surface waves were studied in piezoelectric ceramics with metal surface layer in [14]. The study presented the conditions for the existence of a B-G surface wave and discussed a new surface wave in the piezoelectric structure. Using a formulation of periodic Hamiltonian system, dispersion relations for the propagation of shear waves in piezoelectric layered structures were analyzed in [36,38]. Besides the existence condition for Love-type waves, a new existence condition for shear horizontal surface waves in a layered structure of piezoelectric ceramics was derived in [11,12]. The propagation of quasi-shear horizontal acoustic waves was investigated in lithium niobate plates [13,37]. The propagation characteristics of waves have been discussed in magnetoelectric materials [15], piezoelectric materials [7,20], piezoelectric composite structures [17,18,30], functionally graded piezoelectric material [9] and piezoelectric coupled plates [23,33].

The theory of the scattering process of shear horizontal waves in layered piezoelectric composites in terms of a recursive system of equations involving the piezoelectric impedance was discussed in [19]. The dispersion relations and mode shapes of the deflection and the electric potential of the piezoelectric coupled plate by the use of interdigital transducer (IDT) materials were discussed in [34,35]. The propagation behavior of shear waves in multilayered piezoelectric composites structures was investigated in [24–26]. A shear horizontal wave in metal gratings deposited on piezoelectric bounded plates was investigated and effects of the electromechanical coupling coefficient on width and attenuation of the stop bands were shown [6]. A finite element model was developed to study the effect of porosity on the electromechanical response of porous piezoelectric ceramics [10]. The study on interfacial waves has been extended from piezoelectric materials to a piezoelectric–piezomagnetic bi-material [29]. Constitutive equations for porous piezoelectric materials were derived and vibration characteristics of such a plate were studied [31]. Wave propagations in transversely isotropic porous materials were studied in [32]. Dynamic behavior of wave propagation in layered periodic composites consisting of piezoelectric and piezomagnetic phases have been discussed [21] and the dispersion curves and displacement fields have been characterized [16].

New physical insights into the behavior of periodic systems were obtained by analyzing SH modes in terms of Floquet waves [8]. For guided waves, polarized in the vertical plane in plates of alternating aluminum–epoxy and aramid–epoxy composites, the dispersion and frequency bands do not at all scale with the frequency-thickness product, unlike the behavior expected for a homogeneous plate [28]. The propagation of Floquet waves has been investigated in a composite plate composed of periodic layers together with experimental measurements and demonstrated that transverse resonance can be established only in the Floquet pass bands of the periodic composite [27]. The coupled electro-elastic SH-waves propagating oblique to the lamination of a one-dimensional piezoelectric periodic structure have been studied [22] by using Floquet wave theory, and results demonstrate the significant effect of piezoelectricity on the widths of band gaps. Floquet analysis of the SH-wave propagating in periodically layered plates has been studied [3] and results show that this phenomenon can be attributed to the pass band and stop band structures caused by the layering. The model of periodically layered porous piezoelectric composites has not been studied so far.

In the present work, we consider the propagation of SH-waves in periodically porous piezoelectric layered media. The main aim is to reveal the propagation properties of SH-waves in such new composite materials, and the results obtained are expected to be useful for the analysis and design of such a type of composite acoustic wave devices. The composite structure consists of polymeric layers and porous piezoelectric layers. Frequency equations are derived for the SH-propagation along the direction normal to the layering as well as along the direction of layering. In addition, SH modes in terms of Floquet waves by using Floquet wave theory have also been studied. Two particular materials, that is, Polythene and PZT-5H are taken for the numerical computation. The effects of volume fraction, shear modulus and porosity on phase velocity and stop band effect are discussed.

2 Formulation of the problem

The propagation behavior of horizontally polarized shear waves in a periodic composite structure, as shown in Fig. 1, is taken for the study. The composite structure consists of isotropic polymeric thin films with thickness h_1, bonded perfectly to the transversely isotropic porous piezoelectric thin films with thickness h_2, alternately. The poling direction of the piezoelectric layer is considered along the z-axis, perpendicular to the x–y plane. The propagation direction of SH-waves is considered along the x-axis (the direction normal to the layering) and the y-axis (the direction of the layering), separately. The constitutive equations for the polymeric material

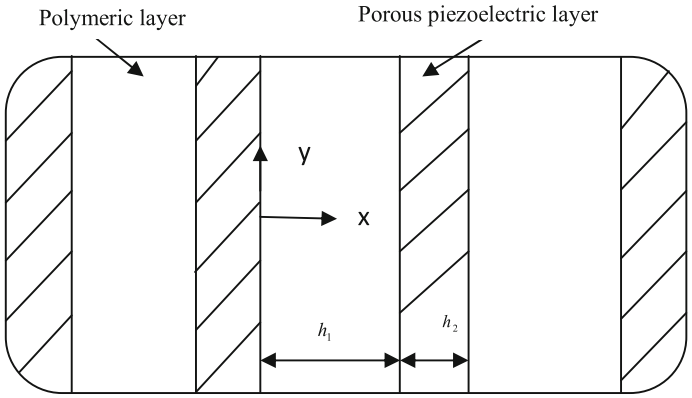

Fig. 1 Piezoceramic layered structure

(M_1) which is treated as isotropic dielectric medium are as follows:

$$\begin{aligned} \sigma'_{ij} &= c'_{ijkl}\varepsilon'_{kl}, \\ D'_i &= \xi'_{ik}E'_k. \end{aligned} \tag{1a}$$

In these equations, σ'_{ij} is the stress tensor, ε'_{ij} is strain tensor, D'_i is electric displacement and E'_i is the electric field for M_1. c'_{ijkl}, ξ'_{kl} are the elastic and dielectric constants.

The constitutive equations for the porous piezoelectric material (M_2) are [31]

$$\begin{aligned} \sigma_{ij} &= c_{ijkl}\varepsilon_{kl} + m_{ij}\varepsilon^* - e_{kij}E_k - \zeta_{kij}E^*_k, \\ \sigma^* &= m_{ij}\varepsilon_{ij} + R\varepsilon^* - \zeta_k E_k - e^*_k E^*_k, \\ D_i &= e_{ikl}\varepsilon_{kl} + \zeta_i\varepsilon^* + \xi_{il}E_l + A_{il}E^*_l, \\ D^*_i &= \zeta_{ikl}\varepsilon_{kl} + e^*_i\varepsilon^* + A_{il}E_l + \xi^*_{il}E^*_l. \end{aligned} \tag{1b}$$

$\sigma_{ij}(\sigma^*)$ and $\varepsilon_{ij}(\varepsilon^*)$ are the stress and strain tensor components for the solid (fluid) phase in M_2. $D_i(D^*_i)$ and $E_i(E^*_i)$ are the electric displacement and electric field vector for the solid (fluid) phase in M_2. Also c_{ijkl}, m_{ij}, R are elastic constants; $e_{ijk}, e^*_i, \zeta_{ijk}, \zeta_i$ are the piezoelectric constants and $\xi_{ij}, \xi^*_{ij}, A_{ij}$ are the dielectric constants.

The equations of motion, in the absence of body forces and surface charge density for M_1 and M_2, are as follows:

$$\begin{aligned} \sigma'_{ij,j} &= \rho'\ddot{u'_i}, \\ D'_{i,i} &= 0, \end{aligned} \tag{2a}$$

and

$$\begin{aligned} \sigma_{ij,j} &= (\rho_{11})_{ij}\ddot{u_j} + (\rho_{12})_{ij}\ddot{U^*_j}, \\ \sigma^*_{,i} &= (\rho_{12})_{ij}\ddot{u_j} + (\rho_{22})_{ij}\ddot{U^*_j}, \\ D_{i,i} &= 0, \\ D^*_{i,i} &= 0, \end{aligned} \tag{2b}$$

where u'_i and ρ' are the mechanical displacement and mass density for M_1, and u_i, U^*_i are the mechanical displacement components of M_2. $(\rho_{11})_{ij}$, $(\rho_{12})_{ij}$, $(\rho_{22})_{ij}$ are dynamical mass coefficients.

Further, we have

$$\varepsilon'_{ij} = \frac{1}{2}(u'_{i,j} + u'_{j,i}), \qquad E'_i = -\phi'_{,i}, \tag{3a}$$

and

$$\begin{aligned} \varepsilon_{ij} &= \tfrac{1}{2}(u_{i,j} + u_{j,i}), \quad & \varepsilon^* &= U^*_{i,i}, \\ E_i &= -\phi_{,i}, & E^*_i &= -\phi^*_{,i}, \end{aligned} \tag{3b}$$

where ϕ' is the electric potential function for M_1, and ϕ (ϕ^*) is the electric potential function for the solid (fluid) phase for M_2.

The constitutive equations for the medium M_1 are

$$\begin{aligned} \sigma'_{11} &= c'_{11}\varepsilon'_{11} + c'_{12}\varepsilon'_{22} + c'_{12}\varepsilon'_{33}, \\ \sigma'_{22} &= c'_{12}\varepsilon'_{11} + c'_{11}\varepsilon'_{22} + c'_{12}\varepsilon'_{33}, \\ \sigma'_{33} &= c'_{12}\varepsilon'_{11} + c'_{12}\varepsilon'_{22} + c'_{11}\varepsilon'_{33}, \\ \sigma'_{32} &= 2c'_{44}\varepsilon'_{32}, \\ \sigma'_{31} &= 2c'_{44}\varepsilon'_{31}, \\ \sigma'_{12} &= 2c'_{44}\varepsilon'_{12}, \\ D'_1 &= \xi'_{11}E'_1, \\ D'_2 &= \xi'_{11}E'_2, \\ D'_3 &= \xi'_{11}E'_3. \end{aligned} \tag{4a}$$

The constitutive equations for the medium M_2 can be written as

$$\begin{aligned} \sigma_{11} &= c_{11}\varepsilon_{11} + c_{12}\varepsilon_{22} + c_{13}\varepsilon_{33} + m_{11}\varepsilon^* - e_{31}E_3, \\ \sigma_{22} &= c_{12}\varepsilon_{11} + c_{11}\varepsilon_{22} + c_{13}\varepsilon_{33} + m_{11}\varepsilon^* - e_{31}E_3, \\ \sigma_{33} &= c_{13}\varepsilon_{11} + c_{13}\varepsilon_{22} + c_{33}\varepsilon_{33} + m_{33}\varepsilon^* - e_{33}E_3, \\ \sigma_{32} &= 2c_{44}\varepsilon_{32} - e_{15}E_2, \\ \sigma_{31} &= 2c_{44}\varepsilon_{31} - e_{15}E_1, \\ \sigma_{12} &= 2c_{66}\varepsilon_{12}, \\ \sigma^* &= m_{11}\varepsilon_{11} + m_{11}\varepsilon_{22} + m_{33}\varepsilon_{33} + R\varepsilon^*, \\ D_1 &= 2e_{15}\varepsilon_{13} + \xi_{11}E_1 + A_{11}E^*_1, \\ D_2 &= 2e_{15}\varepsilon_{23} + \xi_{11}E_2 + A_{11}E^*_2, \\ D_3 &= e_{31}\varepsilon_{11} + e_{31}\varepsilon_{22} + e_{33}\varepsilon_{33} + \zeta_3\varepsilon^* + \xi_{33}E_3 + A_{33}E^*_3, \\ D^*_1 &= A_{11}E_1 + \xi^*_{11}E^*_1, \\ D^*_2 &= A_{11}E_2 + \xi^*_{11}E^*_2, \\ D^*_3 &= e^*_3\varepsilon^* + A_{33}E_3 + \xi^*_{33}E^*_3, \end{aligned} \tag{4b}$$

where $c'_{44} = (c'_{11} - c'_{12})/2$, $c_{66} = (c_{11} - c_{12})/2$.

For an SH-wave propagating in the xy-plane, the mechanical displacements and electric potential functions can be represented as

$$u'_1 = 0, \quad u'_2 = 0, \quad u'_3 = w'(x, y, t), \quad \phi' = \phi'(x, y, t), \tag{5a}$$

and

$$u_1 = 0, \quad u_2 = 0, \quad u_3 = w(x, y, t), \quad U^*_3 = W^*(x, y, t), \quad \phi = \phi(x, y, t), \quad \phi^* = \phi^*(x, y, t). \tag{5b}$$

Using Eqs. (3a)–(5a) in Eq. (2a), we get

$$\begin{aligned} c'_{44}\left(\frac{\partial^2 w'}{\partial x^2} + \frac{\partial^2 w'}{\partial y^2}\right) &= \rho'\frac{\partial^2 w'}{\partial t^2}, \\ \xi'_{11}\left(\frac{\partial^2 \phi'}{\partial x^2} + \frac{\partial^2 \phi'}{\partial y^2}\right) &= 0. \end{aligned} \tag{6a}$$

Similarly, using Eqs. (3b)–(5b) in Eq. (2b) and eliminating U^*_3 and ϕ^*, we get

$$
\begin{aligned}
c_{44}\left(\frac{\partial^2 w}{\partial x^2}+\frac{\partial^2 w}{\partial y^2}\right)+e_{15}\left(\frac{\partial^2 \phi}{\partial x^2}+\frac{\partial^2 \phi}{\partial y^2}\right)&=\rho^p\frac{\partial^2 w}{\partial t^2},\\
e_{15}\left(\frac{\partial^2 w}{\partial x^2}+\frac{\partial^2 w}{\partial y^2}\right)-\xi_{11}^p\left(\frac{\partial^2 \phi}{\partial x^2}+\frac{\partial^2 \phi}{\partial y^2}\right)&=0,
\end{aligned}
\tag{6b}
$$

where $\rho^p=(\rho_{11})_{33}-(\rho_{12})_{33}^2/(\rho_{22})_{33}$, $\xi_{11}^p=\xi_{11}-A_{11}^2/\xi_{11}^*$, $\nabla^2\phi^*=-\frac{A_{11}}{\xi_{11}^*}\nabla^2\phi$.

At the interface $x=0$, the boundary conditions require that normal displacement, shear stress, electrical displacement and electrical potential function should be continuous, that is,

$$
\begin{aligned}
w'(0,y)&=w(0,y),\\
\phi'(0,y)&=\phi(0,y),\\
\sigma_{13}'(0,y)&=\sigma_{13}(0,y),\\
D_1'(0,y)&=D_1(0,y)+D_1^*(0,y).
\end{aligned}
\tag{7a}
$$

The periodicity of the components of the stress, mechanical displacement, electrical displacement and electrical potential function at all interfaces leads to the following conditions:

$$
\begin{aligned}
w'(h1,y)&=w(-h2,y),\\
\phi'(h1,y)&=\phi(-h2,y),\\
\sigma_{13}'(h1,y)&=\sigma_{13}(-h2,y),\\
D_1'(h1,y)&=D_1(-h2,y)+D_1^*(-h2,y).
\end{aligned}
\tag{7b}
$$

3 Solutions

We consider the following two cases for solving Eqs. (6) and (7).

3.1 Wave propagation along the direction normal to the layering

For the composite layered structures, when the SH-waves propagate along the positive direction of the x-axis (along the direction normal to the layering), the solutions of Eqs. (6a) and (6b) can be considered as follows:

$$
\begin{aligned}
w'(x,t)&=W'(x)\exp[ik(x-ct)],\\
\phi'(x,t)&=\Phi'(x)\exp[ik(x-ct)],
\end{aligned}
\tag{8a}
$$

and

$$
\begin{aligned}
w(x,t)&=W(x)\exp[ik(x-ct)],\\
\phi(x,t)&=\Phi(x)\exp[ik(x-ct)],
\end{aligned}
\tag{8b}
$$

where k is the wave number, $i=\sqrt{-1}$, c is the propagation velocity of the SH-waves, $W'(x)$, $W(x)$, $\Phi'(x)$ and $\Phi(x)$ are undetermined functions.

Using Eqs. (8a) and (8b) in Eqs. (6a) and (6b) gives

$$
\begin{aligned}
c_{44}'\left(\frac{\partial^2 W'}{\partial x^2}+2ik\frac{\partial W'}{\partial x}-k^2W'\right)&=-\rho' k^2c^2W',\\
\frac{\partial^2\Phi'}{\partial x^2}+2ik\frac{\partial\Phi'}{\partial x}-k^2\Phi'&=0,
\end{aligned}
\tag{9a}
$$

and

$$
\begin{aligned}
c_{44}\left(\frac{\partial^2 W}{\partial x^2}+2ik\frac{\partial W}{\partial x}-k^2W\right)+e_{15}\left(\frac{\partial^2\Phi}{\partial x^2}+2ik\frac{\partial\Phi}{\partial x}-k^2\Phi\right)&=-\rho^p k^2c^2W,\\
e_{15}\left(\frac{\partial^2 W}{\partial x^2}+2ik\frac{\partial W}{\partial x}-k^2W\right)-\xi_{11}^p\left(\frac{\partial^2\Phi}{\partial x^2}+2ik\frac{\partial\Phi}{\partial x}-k^2\Phi\right)&=0.
\end{aligned}
\tag{9b}
$$

The above equations give

$$\begin{aligned} w'(x,t) &= [A_1 e^{(-1+c/c'_{\mathrm{SH}})ikx} + B_1 e^{(-1-c/c'_{\mathrm{SH}})ikx}] e^{ik(x-ct)}, \\ \phi'(x,t) &= (A'_1 + B'_1 x) e^{-ikx} e^{ik(x-ct)}, \end{aligned} \tag{10a}$$

and

$$\begin{aligned} w(x,t) &= \left[A_2 e^{(-1+c/c_{\mathrm{SH}})ikx} + B_2 e^{(-1-c/c_{\mathrm{SH}})ikx}\right] e^{ik(x-ct)}, \\ \phi(x,t) &= \left[(A'_2 + B'_2 x) e^{-ikx} + \tfrac{e_{15}}{\xi^p_{11}} \left[A_2 e^{(-1+c/c_{\mathrm{SH}})ikx} + B_2 e^{(-1-c/c_{\mathrm{SH}})ikx}\right]\right] e^{ik(x-ct)}, \end{aligned} \tag{10b}$$

where $c'_{\mathrm{SH}} = \sqrt{\frac{c'_{44}}{\rho'}}$ and $c_{\mathrm{SH}} = \sqrt{\frac{P}{\rho^p}}$ are the bulk shear wave velocity in the polymeric layer and the porous piezoelectric layer, respectively, and $P = c_{44} + \frac{e_{15}^2}{\xi^p_{11}}$.

3.2 Wave propagation along the direction of the layering

For the case of the wave propagation along the positive direction of the y-axis (along the direction of layering), we can obtain the solutions of mechanical displacement and electrical potential functions for the polymeric layer and the porous piezoelectric layer as follows:

$$\begin{aligned} w'(x,y,t) &= \left[A_1 e^{-ib_1 x} + B_1 e^{ib_1 x}\right] e^{ik(y-ct)}, \\ \phi'(x,y,t) &= \left[A'_1 e^{-kx} + B'_1 e^{kx}\right] e^{ik(y-ct)}, \end{aligned} \tag{11a}$$

and

$$\begin{aligned} w(x,y,t) &= \left[A_2 e^{-b_2 x} + B_2 e^{b_2 x}\right] e^{ik(y-ct)}, \\ \phi(x,y,t) &= \left[A'_2 e^{-kx} + B'_2 e^{kx} + \tfrac{e_{15}}{\xi^p_{11}} \left(A_2 e^{-b_2 x} + B_2 e^{b_2 x}\right)\right] e^{ik(y-ct)}, \end{aligned} \tag{11b}$$

where $b_1 = k\sqrt{\frac{c^2}{c'^2_{\mathrm{SH}}} - 1}$, $b_2 = k\sqrt{1 - \frac{c^2}{c^2_{\mathrm{SH}}}}$.

4 Dispersion equation

4.1 Wave propagation along the direction normal to the layering

Using Eqs. (10a) and (10b) in Eqs. (4a) and (4b), respectively, we have

$$\begin{aligned} \sigma'_{13} &= \tfrac{ikcc'_{44}}{c'_{\mathrm{SH}}} \left[A_1 e^{(-1+c/c'_{\mathrm{SH}})ikx} - B_1 e^{(-1-c/c'_{\mathrm{SH}})ikx}\right] e^{ik(x-ct)}, \\ D'_1 &= -\xi'_{11} B'_1 e^{-ikx} e^{ik(x-ct)}, \end{aligned} \tag{12a}$$

and

$$\begin{aligned} \sigma_{13} &= \left[e_{15} B'_2 e^{-ikx} + \tfrac{ikcP}{c_{\mathrm{SH}}} \left(A_2 e^{(-1+c/c_{\mathrm{SH}})ikx} - B_2 e^{(-1-c/c_{\mathrm{SH}})ikx}\right)\right] e^{ik(x-ct)}, \\ D_1 &= \left[\tfrac{ikc}{c_{\mathrm{SH}}} \left(e_{15} - l_{11} \tfrac{e_{15}}{\xi^p_{11}}\right) \left(A_2 e^{(-1+c/c_{\mathrm{SH}})ikx} - B_2 e^{(-1-c/c_{\mathrm{SH}})ikx}\right) - l_{11} B'_2 e^{-ikx}\right] e^{ik(x-ct)}, \\ D^*_1 &= -l_{12} \left[\tfrac{ikce_{15}}{\xi^p_{11} c_{\mathrm{SH}}} \left(A_2 e^{(-1+c/c_{\mathrm{SH}})ikx} - B_2 e^{(-1-c/c_{\mathrm{SH}})ikx}\right) + B'_2 e^{-ikx}\right] e^{ik(x-ct)}. \end{aligned} \tag{12b}$$

Making use of the above equations and boundary conditions (7a) and (7b), we obtain the following homogeneous system of linear algebraic equations with unknowns A_1, B_1, A_1', B_1', A_2, B_2, A_2' and B_2':

$$\begin{aligned}
A_1 + B_1 - A_2 - B_2 &= 0,\\
A_1' - A_2' - \tfrac{e_{15}}{\xi_{11}^p} A_2 - \tfrac{e_{15}}{\xi_{11}^p} B_2 &= 0,\\
A_1 - B_1 - \tfrac{e_{15}c_{\mathrm{SH}}'}{ikcc_{44}'} B_2' - QA_2 + QB_2 &= 0,\\
-\xi_{11}' B_1' - \tfrac{ikcl_{13}}{c_{\mathrm{SH}}} A_2 + \tfrac{ikcl_{13}}{c_{\mathrm{SH}}} B_2 + lB_2' &= 0,\\
A_1 e^{i\alpha} + B_1 e^{-i\alpha} - A_2 e^{i(kh-\beta)} - B_2 e^{i(kh+\beta)} &= 0,\\
A_1' + B_1' h_1 - A_2' e^{ikh} + B_2' h_2 e^{ikh} - \tfrac{e_{15}}{\xi_{11}^p} A_2 e^{i(kh-\beta)} - \tfrac{e_{15}}{\xi_{11}^p} B_2 e^{i(kh+\beta)} &= 0,\\
A_1 e^{i\alpha} - B_1 e^{-i\alpha} - \tfrac{e_{15}c_{\mathrm{SH}}'}{ikcc_{44}'} B_2' e^{ikh} - QA_2 e^{i(kh-\beta)} + QB_2 e^{i(kh+\beta)} &= 0,\\
-\xi_{11}' B_1' - \tfrac{ikcl_{13}}{c_{\mathrm{SH}}} A_2 e^{i(kh-\beta)} + \tfrac{ikcl_{13}}{c_{\mathrm{SH}}} B_2 e^{i(kh+\beta)} + lB_2' e^{ikh} &= 0,
\end{aligned} \tag{13}$$

where

$$\begin{aligned}
&l_{11} = \xi_{11} - (A_{11}^2/\xi_{11}^*)C_v, \quad l_{12} = A_{11}(1 - C_v), \quad C_v = c_{\phi^*}^2/c_{\phi}^2,\\
&l_{13} = e_{15}[1 - (l_{11}/\xi_{11}^p) - (l_{12}/\xi_{11}^p)], \quad l = l_{11} + l_{12},\\
&\alpha = (ckh_1)/c_{\mathrm{SH}}', \quad \beta = (ckh_2)/c_{\mathrm{SH}}, \quad Q = (Pc_{\mathrm{SH}}')/(c_{44}'c_{\mathrm{SH}}).
\end{aligned}$$

The non-trivial solution of system (13) exists when

$$\begin{aligned}
\cos(kh) = \cos(\alpha)\cos(\beta) - \frac{(1+Q^2)}{2Q}\sin(\alpha)\sin(\beta)\\
+ \frac{l_{15}}{2Q}[\cos(\alpha) + \cos(\beta) + \cos(\alpha)\cos(\beta) - Q\sin(\alpha)\sin(\beta) - 1 - 2\cos(kh)],
\end{aligned} \tag{14}$$

in which $h = h_1 + h_2$, $l_{14} = (lc_{44}'c_{\mathrm{SH}})/(l_{13}e_{15}c_{\mathrm{SH}}')$, $l_{15} = 1/l_{14}$.

Equation (14) is the dispersion equation of the SH-waves propagating in a periodic piezoelectric composite layered structure along the direction normal to the layering.

4.2 Wave propagation along the direction of the layering

For the case of the SH-wave propagation along the direction of layering, the corresponding stress and electrical displacement components in the polymeric layer and porous piezoelectric layer can be obtained by substituting Eqs. (11a) and (11b) into Eqs. (4a) and (4b) as follows:

$$\begin{aligned}
\sigma_{13}' &= ic_{44}'b_1[-A_1 e^{-ib_1 x} + B_1 e^{ib_1 x}]e^{ik(y-ct)},\\
D_1' &= -\xi_{11}' k[-A_1' e^{-kx} + B_1' e^{kx}]e^{ik(y-ct)},
\end{aligned} \tag{15a}$$

and

$$\begin{aligned}
\sigma_{13} &= [Pb_2(-A_2 e^{-b_2 x} + B_2 e^{b_2 x}) + e_{15}k(-A_2' e^{-kx} + B_2' e^{kx})e^{ik(y-ct)},\\
D_1 &= \left[b_2\left(e_{15} - l_{11}\tfrac{e_{15}}{\xi_{11}^p}\right)(-A_2 e^{-b_2 x} + B_2 e^{b_2 x}) - l_{11}k(-A_2' e^{-kx} + B_2' e^{kx})\right]e^{ik(y-ct)},\\
D_1^* &= -l_{12}[(-kA_2' e^{-kx} + kB_2' e^{kx}) + \tfrac{e_{15}}{\xi_{11}^p}(-b_2 A_2 e^{-b_2 x} + b_2 B_2 e^{b_2 x})]e^{ik(y-ct)}.
\end{aligned} \tag{15b}$$

Using the above equations and the boundary conditions (7a) and (7b), we get

$$2e_{15}^2\frac{\xi'_{11}}{\xi_{11}^p}[(c'_{44}q_1T_1F_2+Pq_2S_1G_2)(\xi'_{11}M_1N_2+lM_2N_1)-(c'_{44}q_1F_2+Pq_2S_1)$$
$$\times(\xi'_{11}M_1+lM_2)+l_{13}e_{15}q_2S_1M_2(1-G_2N_1)]-e_{15}^4\left(\frac{\xi'_{11}}{\xi_{11}^p}\right)^2S_1F_2M_2M_1$$
$$-[(P^2q_2^2-c'^2_{44}q_1^2)S_1F_2+2Pc'_{44}q_1q_2(T_1G_2-1)][(l^2+\xi'^2_{11})M_1M_2+2(N_1N_2-1)l\xi'_{11}]$$
$$+l_{13}e_{15}q_2[2P\xi'_{11}S_1F_2q_2(1-N_1N_2)+2lc'_{44}q_1M_1M_2(1-T_1G_2)-4\xi'_{11}c'_{44}q_1(1-N_1N_2)$$
$$\times(1-T_1G_2)-(l_{13}e_{15}q_2+2Plq_2)S_1M_1M_2F_2]=0, \tag{16}$$

where $q_1=\sqrt{\frac{c^2}{c'^2_{\mathrm{SH}}}-1}$, $q_2=\sqrt{1-\frac{c^2}{c^2_{\mathrm{SH}}}}$ and $F_2, G_2, M_1, N_1, M_2, N_2, S_1, T_1$ are given in Appendix A.

Equation (16) is the dispersion equation of SH-waves propagating in the periodic porous/piezoelectric layered structure along the direction of layering. It is readily seen from the phase velocity equations (14) and (16) that the phase velocity c is related to wave number, layer thickness, elastic, dielectric and piezoelectric constants.

5 Reduced case

In this section, the dispersion equations (14) and (16) are reduced for the piezoelectric case. For the case of SH-waves propagating along the direction normal to the layering, when $l_{15}=0$, that is, the porous piezoelectric media becomes piezoelectric, Eq. (14) reduces to

$$\cos(kh)=\cos(\alpha)\cos(\beta)-\frac{(1+Q^2)}{2Q}\sin(\alpha)\sin(\beta), \tag{17}$$

which is the dispersion relation for an SH-wave propagating in a periodic piezoelectric layered structure along the direction normal to the layering [24].

For the case of an SH-wave propagating along the direction of layering, when $l_{13}=0$, Eq. (16) reduces to

$$2e_{15}^2\frac{\xi'_{11}}{\xi_{11}^p}[(c'_{44}q_1T_1F_2+Pq_2S_1G_2)(\xi'_{11}M_1N_2+lM_2N_1)-(c'_{44}q_1F_2+Pq_2S_1)$$
$$\times(\xi'_{11}M_1+lM_2)]-e_{15}^4\left(\frac{\xi'_{11}}{\xi_{11}^p}\right)^2S_1F_2M_2M_1-[(P^2q_2^2-c'^2_{44}q_1^2)S_1F_2$$
$$+2Pc'_{44}q_1q_2(T_1G_2-1)][(l^2+\xi'^2_{11})M_1M_2+2(N_1N_2-1)l\xi'_{11}]=0, \tag{18}$$

which is the dispersion relation for an SH-wave propagating in a periodic piezoelectric layered structure along the direction of layering [24].

6 Floquet wave

Floquet modes are characteristic modes for an infinite periodically layered medium. It is shown in [27] that Floquet modes can be utilized to significantly simplify the solution to the plate wave problems in the presence of periodic structures. Following this and the methodology used in [22], we study the propagation of Floquet wave in the periodic piezoceramic layered structure in the present section.

The boundary conditions at the interface $x=0$ are similar as in the case of SH-waves, whereas at $x=-h_2$, the wave must satisfy Bloch–Floquet quasi-periodicity conditions [27] which are given as

$$\begin{aligned}
w'(h1,y)&=\lambda w(-h2,y),\\
\phi'(h1,y)&=\lambda\phi(-h2,y),\\
\sigma'_{13}(h1,y)&=\lambda\sigma_{13}(-h2,y),\\
D'_1(h1,y)&=\lambda[D_1(-h2,y)+D_1^*(-h2,y)],
\end{aligned} \tag{19}$$

Table 1 Material constants

Materials	Elastic constants (10^{10}N/m^2)	Piezoelectric constants (C/m^2)	Dielectric constants (10^{-10}F/m)	Mass density (kg/m^3)
Polythene	$c'_{44} = 0.128$	–	$\xi'_{11} = 0.2036$	$\rho' = 1{,}180$
PZT-5H	$c_{44} = 2.3$	$e_{15} = 17$	$\xi_{11} = 277$	$(\rho_{11})_{33} = 4{,}950$
			$\xi^*_{11} = 299$	$(\rho_{12})_{33} = -1{,}125$
			$A_{11} = 112$	$(\rho_{22})_{33} = 4{,}800$

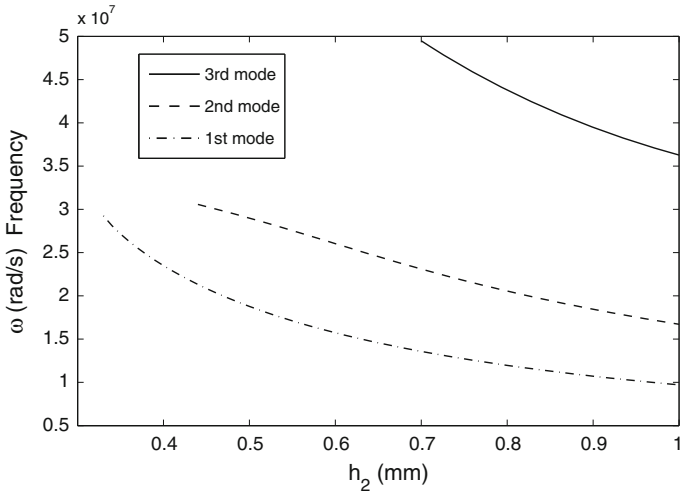

Fig. 2 Variation of ω with h_2 for $c = 1{,}500\,\mathrm{m/s}$, $h_1 = 0.1\,\mathrm{mm}$

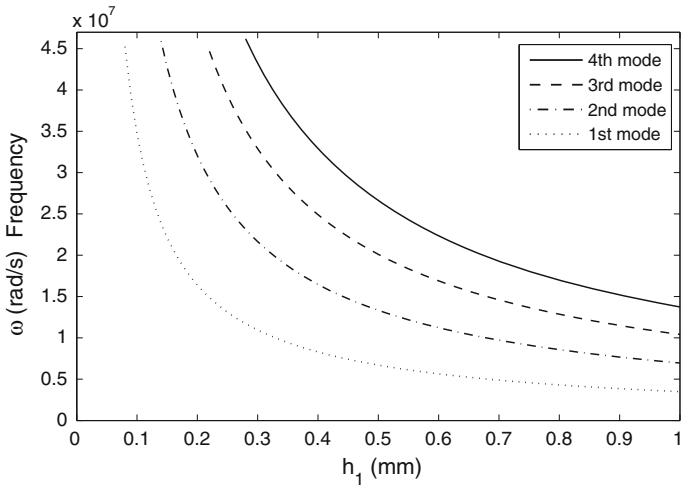

Fig. 3 Variation of ω with h_1 for $c = 1{,}500\,\mathrm{m/s}$, $h_2 = 0.1\,\mathrm{mm}$

where $\lambda = e^{i\gamma h}$, γ is a component of wave vector called Bloch–Floquet wave number. Making use of Eqs. (11a), (11b), (15a) and (15b) in boundary conditions (7a) and (19) and after simplifications, we obtain

$$\lambda^2 + \frac{d_2}{d_1}\lambda - \frac{d_3}{d_1} = 0, \tag{20}$$

where d_1, d_2, d_3 are given in the Appendix B, and Eq. (20) is the dispersion relation for Floquet wave propagating in a periodic piezoelectric layered structure along the direction of layering.

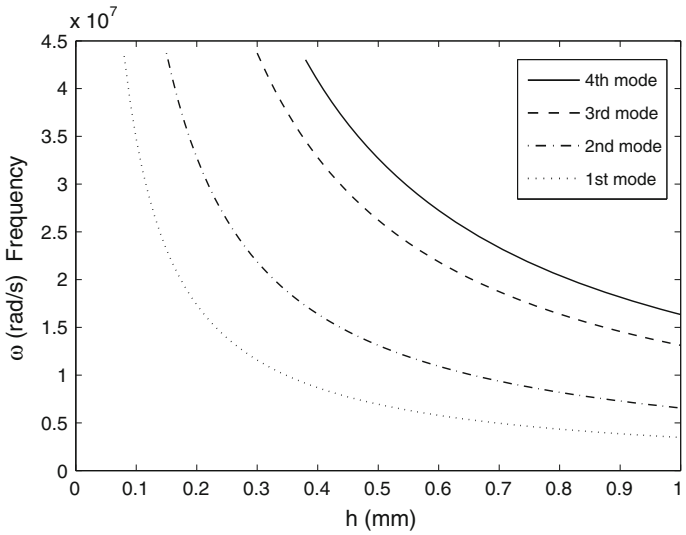

Fig. 4 Variation of ω with h for $c = 1{,}500\,\mathrm{m/s}$, $h_1 = h_2 = h$

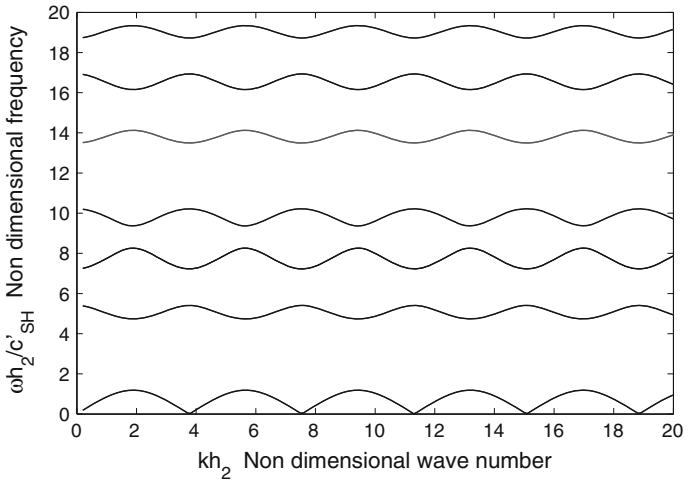

Fig. 5 Variation of $\omega h_2/c'_{\mathrm{SH}}$ with kh_2 for wave propagation in the direction normal to the layering for $r = 0.4$

If the wave propagates normal to the layering ($k = 0$), the dispersion equation (20) becomes

$$\cos(\gamma h) = \cos(\alpha)\cos(\beta) - \frac{(1 + Q^2 + l_{15}Q)}{2(Q + l_{15})}\sin(\alpha)\sin(\beta), \tag{21}$$

which is the dispersion relation for a Floquet wave propagating in a periodic piezoelectric layered structure along the direction normal to the layering.

7 Numerical examples and discussions

In the previous section, analytical solutions of the phase velocity for the SH-wave propagation in the periodic porous piezoelectric layered structure have been obtained. Based on the dispersion equations (14) and (16), numerical computations are performed to illustrate the results of dispersion characteristics. There exists the relationship $\omega = kc$ for the wave velocity c, wave number k and circular frequency ω. To study the propagation behavior of SH-waves in this kind of structure, the polymeric material is considered as polythene, and PZT-5H

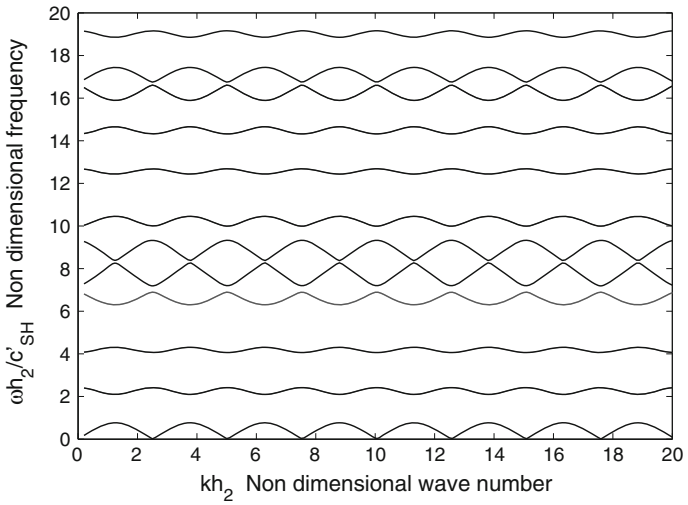

Fig. 6 Variation of $\omega h_2/c'_{\mathrm{SH}}$ with kh_2 for wave propagation in the direction normal to the layering for $r = 0.6$

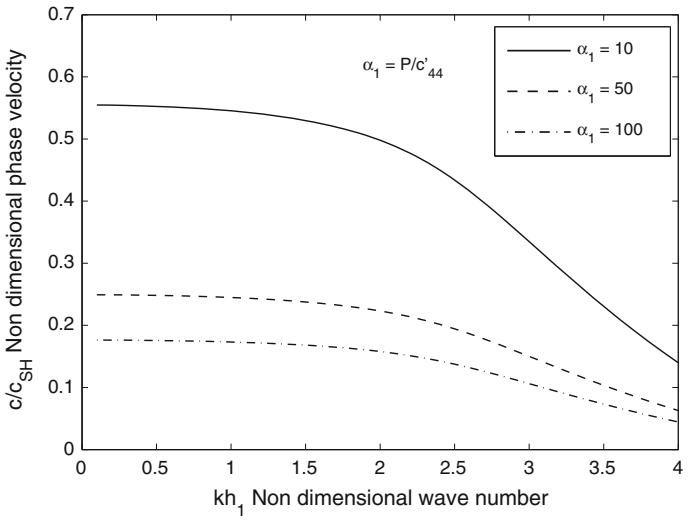

Fig. 7 Variation of c/c_{SH} with kh_1 of wave propagation in the direction normal to the layering for $\alpha_1 = 10$, $\alpha_1 = 50$, $\alpha_1 = 100$. and $r = 0.8$

as porous piezoelectric material. The value of the constant C_v is taken as 0.02752. The material constants taken for numerical computations are given in the Table 1. Some of these material constants are taken from [24].

For the case of wave propagation along the direction normal to the layering, the variation of the wave frequency with the thickness of layers is computed for a specified value of phase velocity c. The value of c for computation purposes is considered as 1,500 m/s. This variation is shown in Figs. 2, 3 and 4. In Fig. 2, h_1 is treated as constant and in Fig. 3, h_2 is treated as constant. In Fig. 4, both h_1 and h_2 are taken to be equal. It is observed that the wave frequency decreases sharply with an increase in thickness of the layer.

The volume fraction of a polythene layer is defined as $r = \frac{h_1}{h_1+h_2}$. We study the variation patterns of the two variables $\omega h_2/c'_{\mathrm{SH}}$ and kh_2 for two values $r = 0.4$ and $r = 0.6$ of the volume fraction, and result are shown in Figs. 5 and 6. It can be seen that the number of stop bands increases with increasing volume fraction r, while the width of the successive stop band decreases. For the case of SH-wave propagation along the direction of layering, there exist no curves similar to Figs. 5 and 6. The fact also indicates that no stop band or filter wave effect exists for that case.

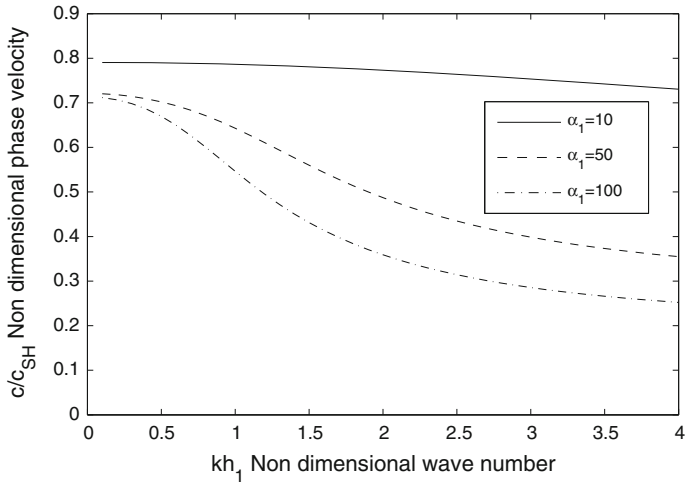

Fig. 8 Variation of c/c_{SH} with kh_1 of wave propagation in the direction of layering for $\alpha_1 = 10$, $\alpha_1 = 50$, $\alpha_1 = 100$ and $r = 0.8$

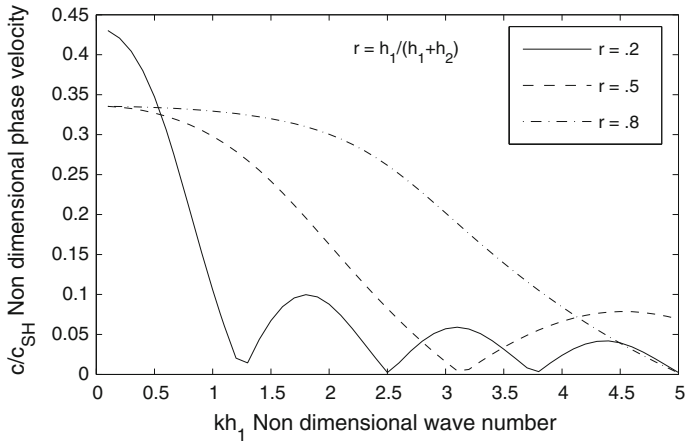

Fig. 9 Variation of c/c_{SH} with kh_1 of wave propagation in the direction normal to layering for $r = 0.2$, $r = 0.5$, $r = 0.8$

For the case of wave propagation along the direction normal to the layering, the variation pattern of the non-dimensional phase velocity c/c_{SH} versus the non-dimensional wave number kh_1 is shown in Fig. 7 for different ratios of shear modulus ($\alpha_1 = P/c'_{44}$) in the PZT-5H ceramic layer to that of the polythene layer for $r = 0.8$. The factor $P = c_{44} + \frac{e_{15}^2}{\xi_{11}^P}$ can be regarded as the effective modulus of the PZT-5H ceramic layer. In case of SH-wave propagation along the direction of the layering, the variation pattern of non-dimensional phase velocity c/c_{SH} versus non-dimensional wave number kh_1 is shown in Fig. 8 for different values of the parameter α_1. It can be noticed from Figs. 7 and 8 that, although the phase velocity decreases with non-dimensional wave number kh_1 in both cases, the variation pattern is different. In case of propagation direction along layering, it decreases steadily with kh_1. However, in case of direction normal to layering, the change is noticeable for large values of kh_1, that is, for high frequency waves, the effect of the shear modulus is less dominant than in case of comparative lower frequency waves.

To study the effect of volume fraction, the phase velocity is computed for different values of kh_1 and is shown in Figs. 9 and 10 for the above-mentioned two cases. As expected, the effect of volume fraction (r) is important when we consider the waves propagating along the direction normal to the layering, as shown in Fig. 9. The nodal points decrease when r increases. In the other case (Fig. 10), the phase velocity decreases with an increase of kh_1 and the stop band effect is not observed in this case.

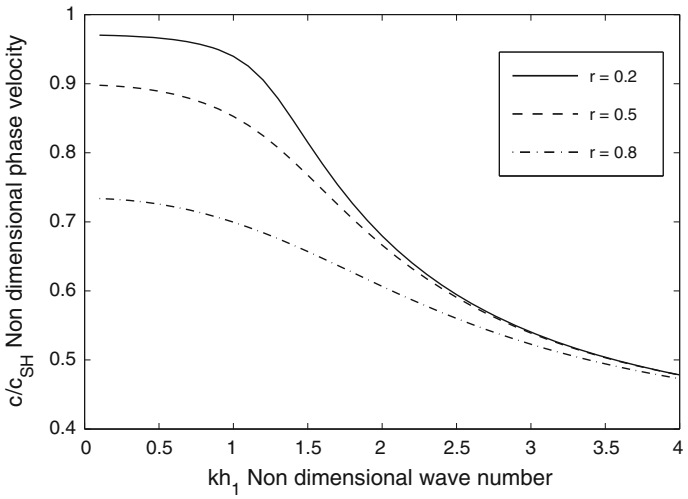

Fig. 10 Variation of c/c_{SH} with kh_1 of wave propagation in the direction of layering for $r = 0.2, r = 0.5, r = 0.8$

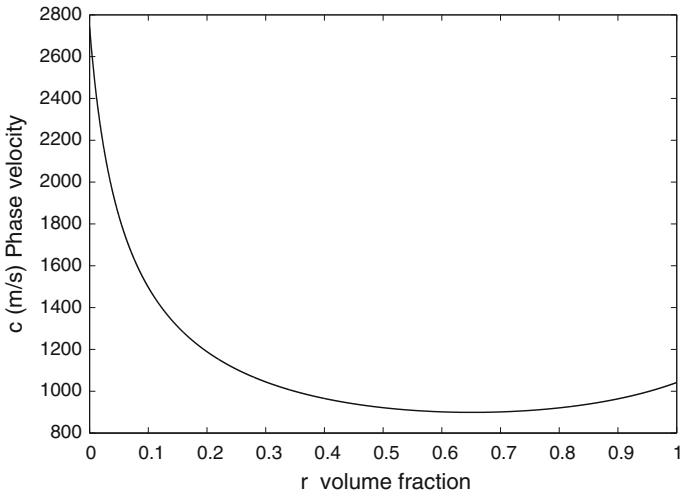

Fig. 11 Variation of c with r of wave propagation in the direction normal to the layering for $\omega = 1{,}000\,\mathrm{Hz}$, $h_1 = 1\,\mathrm{mm}$

Further, the effect of volume fraction on the phase velocity for specified values of frequency and polythene layer thickness is shown in Figs. 11 and 12. The values of the phase velocity at the extreme ends ($r = 0$ and $r = 1$) correspond to the cases when h_2 is very large in comparison with h_1 and when h_2 is zero, respectively. It is seen from Fig. 11 that the phase velocity is smaller than the bulk shear wave velocity in the polythene medium, when volume fraction ranges from 0.303 to 1. It is also seen from Fig. 12 that for the case of the SH-wave propagating along the direction of the layering, the phase velocity of SH-waves satisfies the following expression: $c'_{\mathrm{SH}} < c < c_{\mathrm{SH}}$.

To determine the effect of porosity on phase velocity, the non-dimensional phase velocity is calculated separately for shear modulus $\alpha_1 = 50$, $r = 0.8$ for both piezoelectric and porous piezoelectric media. Its variation with kh_1 along the direction normal to the layering and along the layering is shown in Figs. 13 and 14, respectively.

The stop band and pass band gaps for the Floquet wave propagating normal to the layering are shown in the Figs. 15 and 16. for $r = 0.4$ and $r = 0.6$, respectively. The effect of porosity on stop band and pass band gaps are also observed. It is observed that the number of stop band and pass bands increases with increasing volume fraction. For a particular value of volume fraction, the porosity factor has a small effect on the first band gap width while the width of the second band gap decreases in case of periodic porous piezoelectric

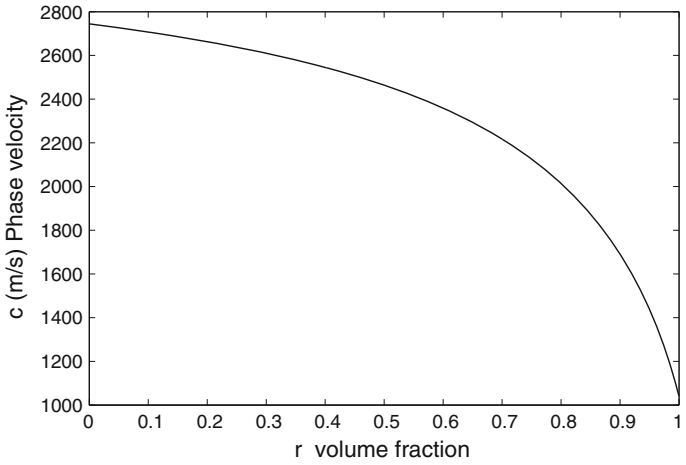

Fig. 12 Variation of c with r of wave propagation in the direction of layering for $\omega = 1{,}000\,\text{Hz}$, $h_1 = 1\,\text{mm}$

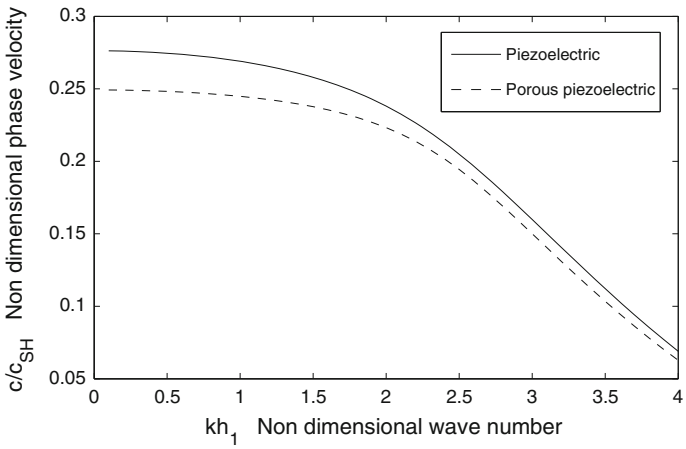

Fig. 13 Variation of c/c_{SH} with kh_1 of wave propagation in the direction normal to the layering of piezoelectric and porous piezoelectric media for $r = 0.8$ and $\alpha_1 = 50$

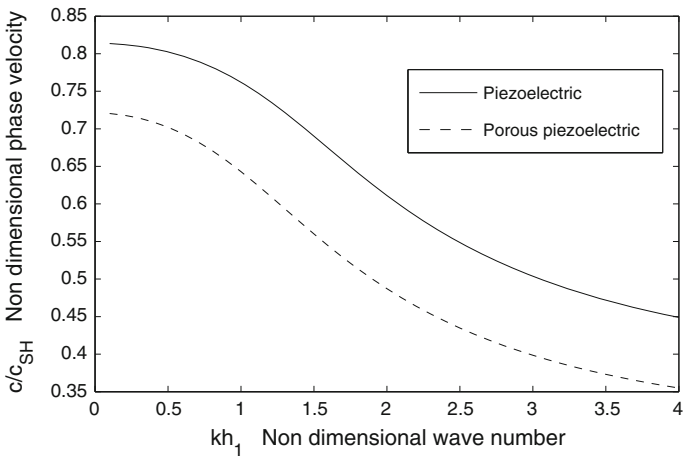

Fig. 14 Variation of c/c_{SH} with kh_1 of wave propagation in the direction of layering of piezoelectric and porous piezoelectric media for $r = 0.8$ and $\alpha_1 = 50$

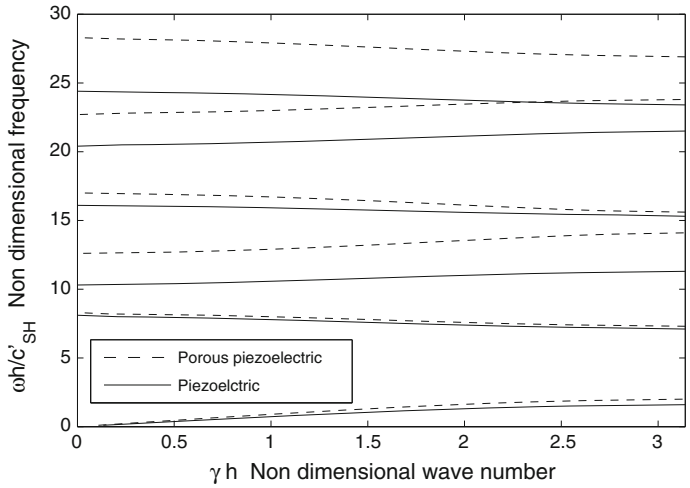

Fig. 15 Variation of $\omega h/c'_{\mathrm{SH}}$ with γh for Floquet wave propagating in the direction normal to the layering of piezoelectric and porous piezoelectric media for $r = 0.4$

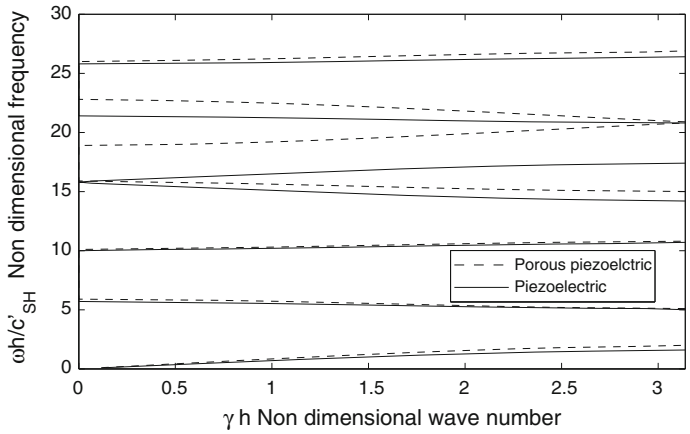

Fig. 16 Variation of $\omega h/c'_{\mathrm{SH}}$ with γh for Floquet wave propagating in the direction normal to the layering of piezoelectric and porous piezoelectric media for $r = 0.6$

structures, shown in Figs. 15 and 16. Figure 17 depicts the variation of phase velocity of a Floquet wave with non-dimensional wave number for different values of volume fraction. It is observed that the phase velocity decreases exponentially with increasing wave number and becomes almost constant after $kh = 3.5$. The phase velocity of the Floquet wave decreases with increasing volume fraction. The effect of porosity on the dispersion curve of the Floquet wave is observed in Fig. 18. The phase velocity of the Floquet wave propagating in the porous piezoelectric periodic layered structure is less in comparison with the periodic piezoelectric structure.

8 Conclusions

The phase velocity equations of SH-wave propagation in the periodic porous piezoelectric layered structure are obtained for the case of waves propagating along the direction of the layering and normal to the layering, respectively. The conclusions are obtained as follows: For shear horizontal waves propagating along the direction normal to the layering,

(i) The phase velocity decreases with increasing wave number for fixed shear modulus.
(ii) The phase velocity of the wave is smaller than c_{SH} when the volume fraction of the polythene layer ranges from 0.303 to 1.

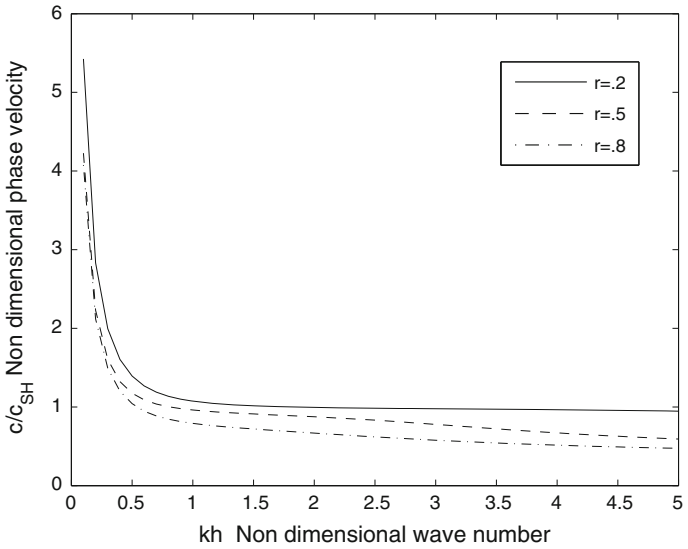

Fig. 17 Variation of c/c_{SH} with kh of Floquet wave propagating in the direction of layering for $r = 0.2, r = 0.5, r = 0.8$. and $\gamma h = 1$

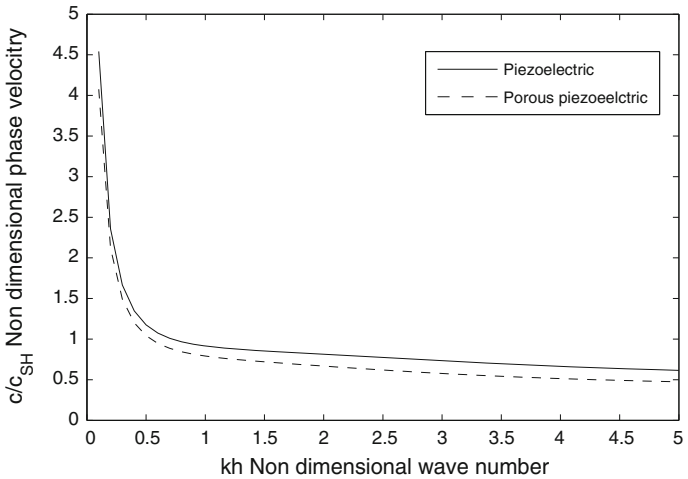

Fig. 18 Variation of c/c_{SH} with kh of Floquet wave propagating in the direction of layering of piezoelectric and porous piezoelectric media for $r = 0.8$ and $\gamma h = 1$

(iii) The number of stop bands increase with increasing magnitude of volume fraction r, while the width of the individual stop band decreases. So such a kind of structure has the potential of being applied to vibration insulation of mechanical devices. Theoretically speaking, when the wave propagates in the direction normal to the layering, by selecting the proper volume fraction of the two materials and adjusting the frequency of vibration within the stop bands, we can yield the effect of vibration insulation.

For SH-waves propagate along the direction of the layering,

(i) The phase velocity decreases with increasing wave number for fixed volume fraction r.
(ii) There exist no stop band effects, that is, no wave filter effect exists.
(iii) The phase velocity of the wave exists in the range $c'_{\mathrm{SH}} < c < c_{\mathrm{SH}}$.

The stop band and pass band effects of the Floquet wave are observed. The number of stop and pass bands increases with increasing volume fraction. The phase velocity of the Floquet wave decreases with increasing

wave number. In addition, the phase velocity becomes small as the porosity is introduced in the piezoelectric media for both SH and Floquet waves propagating along the direction normal to the layering as well as along the direction of layering.

Acknowledgments One of the authors, Mr. Ashok Dahiya, is greatly thankful to the Council of Scientific and Industrial Research for the financial support with grant no. 09/105(0162)/2008-*EMR-I*.

Appendix A

$$\begin{aligned} F_2 &= \sinh(b_2h_2), \quad & G_2 &= \cosh(b_2h_2),\\ M_1 &= \sinh(kh_1), & N_1 &= \cosh(kh_1),\\ M_2 &= \sinh(kh_2), & N_2 &= \cosh(kh_2),\\ S_1 &= \sin(b_1h_1), & T_1 &= \cos(b_1h_1). \end{aligned}$$

Appendix B

$$\begin{aligned}
a_1 &= 2e_{15}^2\frac{\xi_{11}'}{\xi_{11}^p}, \quad a_2 = l_{13}e_{15}q_2,\\
d_{11} &= c_{44}'q_1T_1F_2 + Pq_2S_1G_2, \quad d_{12} = a_1[d_{11} - c_{44}'lq_1F_2M_2 - a_2S_1M_2G_2N_1],\\
d_{13} &= a_1[c_{44}'\xi_{11}'q_1F_2M_1 + Plq_2S_1M_2 - a_2S_1M_2], \quad d_{14} = a_1Pq_2\xi_{11}'S_1M_1,\\
d_{15} &= e_{15}^4\left(\frac{\xi_{11}'}{\xi_{11}^p}\right)^2 S_1F_2M_2M_1, \quad d_{16} = (P^2q_2^2 - c_{44}'^2q_1^2)S_1F_2 + 2Pc_{44}'q_1q_2T_1G_2,\\
d_{17} &= (l^2 + \xi_{11}'^2)M_1M_2 + 2l\xi_{11}'N_1N_2,\\
d_{18} &= a_2[2P\xi_{11}'q_2S_1F_2N_1N_2 + 2lc_{44}'q_1M_1M_2T_1G_2 + 4\xi_{11}'c_{44}'q_1N_1N_2T_1G_2\\
&\qquad + (l_{13}e_{15}q_2 + 2Plq_2)S_1M_1M_2F_2],\\
d_{19} &= a_2[2P\xi_{11}'q_2S_1F_2 + 2lc_{44}'q_1M_1M_2 + 4\xi_{11}'c_{44}'q_1N_1N_2 + 4\xi_{11}'c_{44}'q_1T_1G_2], \quad d_{20} = 4a_2\xi_{11}'c_{44}'q_1,\\
d_{21} &= 2ld_{16}\xi_{11}' + 2Pd_{17}c_{44}'q_1q_2, \quad d_{22} = 4Pl\xi_{11}'c_{44}'q_1q_2,\\
d_1 &= d_{12} - d_{15} - d_{18} - d_{16}d_{17}, \quad d_2 = d_{19} - d_{13} + d_{21} \qquad d_3 = d_{14} + d_{20} + d_{22}.
\end{aligned}$$

References

1. Auld, B.A.: Acoustic Fields and Waves in Solids I. Wiley, New York (1973)
2. Auld, B.A.: Acoustic Fields and Waves in Solids II. Wiley, New York (1973)
3. Auld, B.A., Chimenti, D.E., Shull, P.J.: A Floquet analysis of SH wave propagation in periodically layered composite plates. In: Thompson, D.O., Chimenti, D.E. (eds.) Review of Progress in Quantitative NDE Vol. 1, pp. 227–234. Plenum, New York (1993)
4. Cady, W.G.: Piezoelectricity. McGraw-Hill, NewYork (1946)
5. Christensen, R.M.: Mechanics of Composite Materials. Wiley-Interscience, New York (1979)
6. Chen, S., Tang, T.T., Wang, Z.H.: Shear-horizontal acoustic wave propagation in piezoelectric bounded plates with metal gratings. J. Acoust. Soc. Am. **117**(6), 3609–3615 (2005)
7. Darinskii, A.N., Lyubimov, V.N.: Shear interfacial waves in piezoelectrics. J. Acoust. Soc. Am. **106**(6), 3296–3304 (1999)
8. Datta, S.K., Shah, A.H.: Elastic Waves in Composite Media and Structures. CRC Press/Taylor and Francis, New York (2009)
9. Du, J., Xian, K., Yong, Y.K., Wang, J.: SH-SAW propagation in layered functionally graded piezoelectric material structures loaded with viscous liquid. Acta Mech. **212**(3-4), 271–281 (2010)
10. Gupta, R.K., Venkatesh, T.A.: Electromechanical response of porous piezoelectric materials. Acta Mater. **54**(15), 4063–4078 (2006)
11. Hanhua, F., Xingjiao, L.: Shear-horizontal surface waves in the layered structure. Ultrason. Symp. **1**, 415–418 (1991)
12. Hanhua, F., Xingjiao, L.: Shear-horizontal surface waves in a layered structure of piezoelectric ceramics. IEEE Trans. Ultrason. Ferroelectr. Freq. Control **40**(2), 167–170 (1993)
13. Jin, Y., Joshi, S.G.: Propagation of quasi-shear horizontal acoustic waves in Z-X lithium niobate plates. IEEE Trans. Ultrason. Ferroelectr. Freq. Control **43**(3), 491–494 (1996)

14. Kielczynski, P.J., Pajewski, W., Szalewski, M.: Shear-horizontal surface waves on piezoelectric ceramics with depolarised surface layer. IEEE Trans. Ultrason. Ferroelectr. Freq. Control **36**(2), 287–293 (1989)
15. Liu, J., Fang, D., Liu, X.: A shear horizontal surface wave in magnetoelectric materials. IEEE Trans. Ultrason. Ferroelectr. Freq. Control **54**(7), 1287–1289 (2007)
16. Liu, J., Wei, W., Fang, D.: Propagation behaviors of shear horizontal waves in piezoelectric-piezomagnetic periodically layered stryctures. Acta Mech. Solida Sin. **23**(1), 77–84 (2010)
17. Minagawa, S.: Propagation of harmonic waves in a layered elasto-piezoelectric composite. Mech. Mater. **19**(2–3), 165–170 (1995)
18. Mesquida, A.A., Otero, J.A., Ramos, R.R., Comas, F.: Wave propagation in layered piezoelectric structures. J. Appl. Phys. **83**(9), 4652–4659 (1998)
19. Mesquida, A.A., Ramos, R.R., Comas, F., Monsivais, G., Sirvent, R.: Scattering of shear horizontal piezoelectric waves in piezocomposite media. J. Appl. Phys. **89**(5), 2886–2892 (2001)
20. Nayfeh, A.H., Faidi, W., Abdelrahman, W.: An approximate model for wave propagation in piezoelectric materials. J. Appl. Phys. **85**(4), 2337–2346 (1999)
21. Pang, Y., Liu, J.X., Wang, Y.S., Fang, D.N.: Wave propagation in piezoelectric/piezomagnetic layered periodic composites. Acta Mech. Solida Sin. **21**(6), 483–490 (2008)
22. Piliposian, G.T., Avetisyan, A.S., Ghazaryan, K.B.: Shear wave propagation in periodic phononic/photonic piezoelectric medium. Wave Motion **49**, 125–134 (2012)
23. Quek, S.T., Wang, Q.: On dispersion relations in piezoelectric coupled plate structures. Smart Mater. Struct. **9**(6), 859–867 (2000)
24. Qian, Z., Jin, F., Wang, Z., Kishimoto, K.: Dispersion relations for SH-wave propagation in periodic piezoelectric composite layered structures. Int. J. Eng. Sci. **42**, 673–689 (2004)
25. Qian, Z., Jin, F., Kishimoto, K., Wang, Z.: Effect of initial stress on the propagation behavior of SH-waves in multilayered piezoelectric composite structures. Sens. Act. A. **112**, 368–375 (2004)
26. Qian, Z., Jin, F., Wang, Z., Kishimoto, K.: Investigation of scattering of elastic waves by cylinders in 1-3 piezocomposites. Ultrasonics **43**, 822–831 (2005)
27. Safaeinli, A., Chimenti, D.E.: Floquet analysis of guided waves in periodically layered composites. J. Acoust. Soc. Am. **98**(4), 2336–2342 (1995)
28. Shull, P.J., Chimenti, D.E., Datta, S.K.: Elastic guided waves and the Floquet concept in periodically layered plates. J. Acoust. Soc. Am. **95**(1), 99–108 (1994)
29. Soh, A.K., Liu, J.X.: Interfacial shear horizontal waves in a piezoelectric-piezomagnetic bi-material. Philos. Mag. Lett. **86**, 31–35 (2006)
30. Yang, J.S.: Shear horizontal vibrations of a piezoelectric/ferroelectric wedge. Acta Mech. **173**(1-4), 13–17 (2004)
31. Vashishth, A.K., Gupta, V.: Vibrations of porous piezoelectric ceramic plate. J. Sound Vib. **325**, 781–797 (2009)
32. Vashishth, A.K., Gupta, V.: Wave propagation in transversely isotropic porous piezoelectric materials. Int. J. Solids Struct. **46**, 3620–3632 (2009)
33. Wang, Q., Quek, S.T.: Dispersion relations in piezoelectric coupled beams. AIAA J. **38**(12), 2357–2361 (2000)
34. Wang, Q., Varadan, V.K.: Wave propagation in piezoelectric coupled plates by use of interdigital transducer. Part I: Dispersion characteristics. Int. J. Solids Struct. **39**, 1119–1130 (2002)
35. Wang, Q., Varadan, V.K.: Wave propagation in piezoelectric bounded plates by use of interdigital transducer. Part II: Wave excitation by interdigital transducer. Int. J. Solids Struct. **39**, 1131–1144 (2002)
36. Zinchuk, L.P., Podllipenets, A.N., Shulaga, N.A.: Construction of dispersion equation for electro-elastic shear wave in layered periodic media. Sov. Appl. Mech. **27**(11), 89–93 (1990)
37. Zaitsev, B.D., Joshi, S.G., Kuznetsova, I.E.: Investigation of quasi-shear horizontal acoustic waves in thin plates of lithium niobate. Smart Mater. Struct. **6**, 739–744 (1997)
38. Zinchuk, L.P., Podlipenets, A.N.: Propagation of shear waves in piezoelectric superlattice-substrate structures. J. Math. Sci. **101**(6), 3688–3693 (2000)